



# Optical properties and visible-light driven photocatalytic performance of $\text{Bi}_{14}\text{MoO}_{24}$ semiconductor with layered $\delta\text{-Bi}_2\text{O}_3$ -type structure

Zuoshan Wang<sup>a</sup>, Pengjie Huang<sup>b</sup>, Min Zheng<sup>b,\*</sup>

<sup>a</sup> State and Local Joint Engineering Laboratory for Novel Functional Polymeric Materials, College of Chemistry, Chemical Engineering and Materials Science, Soochow University, Suzhou 215123, China

<sup>b</sup> College of Textile and Clothing Engineering, Soochow University, Suzhou 215006, China

## ARTICLE INFO

### Article history:

Received 1 December 2016

Received in revised form 23 January 2017

Accepted 17 February 2017

### Keywords:

Semiconductors  
Bismuth oxide  
Luminescence  
Solar materials  
Photocatalysis

## ABSTRACT

The bismuth molybdate oxide of  $\text{Bi}_{14}\text{MoO}_{24}$  ( $7\text{Bi}_2\text{O}_3 \cdot \text{MoO}_3$ ) was synthesized by the co-precipitation route. The samples developed into the uniform nanoparticles around 50 nm. Crystalline phase was verified via Rietveld XRD structural refinement. Tetragonal  $\text{Bi}_{14}\text{MoO}_{24}$  is related to that the face-centered cubic (fcc)  $\delta$ -phase of  $\text{Bi}_2\text{O}_3$ -like structure. It has more loose space with a big structure-openness than parent  $\delta\text{-Bi}_2\text{O}_3$ . The surface microstructure and components of the photocatalysts were studied by TEM, SEM, BET, EDS and XPS measurements. The UV–vis absorption spectra showed that the band gap energy of  $\text{Bi}_{14}\text{MoO}_{24}$  was greatly reduced in comparison with  $\delta\text{-Bi}_2\text{O}_3$ . The result confirms that  $\text{Bi}_{14}\text{MoO}_{24}$  can response to visible wavelength between 200 and 500 nm ( $E_g = 6.2 - 2.48$  eV).  $\text{Bi}_{14}\text{MoO}_{24}$  derived from  $\delta\text{-Bi}_2\text{O}_3$  by incorporating Mo ( $7\text{Bi}_2\text{O}_3 \cdot \text{MoO}_3$ ) in the lattices possesses broader conduction band. This greatly benefits the mobility of the light-induced charges taking part in the photocatalytic reactions.  $\text{Bi}_{14}\text{MoO}_{24}$  nanoparticles possess efficient photodegradation on Rhodamine B (RhB) dye and phenol solutions. The photocatalysis activities and mechanisms were discussed on the crystal structure characteristics and the measurements such as photoluminescence, exciton lifetime and XPS results. The layered Bi–O polyhedral structure, good photo-absorption, multivalent elements, quenched luminescence and long exciton lifetime were possibly the origin of its high photocatalytic activity in the photo-degradation.

© 2017 Elsevier B.V. All rights reserved.

## 1. Introduction

Bismuth oxide ( $\text{Bi}_2\text{O}_3$ ) is one of the most widely reported photocatalysts, which has been intensively investigated for preparation methods, electronic structure, wastewater treatment, organic contaminants decomposition,  $\text{CO}_2$  reduction, water splitting under visible-light irradiation, etc. Firstly,  $\text{Bi}_2\text{O}_3$  has suitable band gap (2.1–2.8 eV) responsive to visible light [1,2].  $\text{Bi}^{3+}$  ion has a  $d^{10}$  configuration with a peculiar  $6s^2$  lone pair inducing more internal polar electric field, which promotes charge separations because that holes and electrons present opposite movements in the electric field. Meanwhile, there is high hybridization between Bi-6s and O-2p orbitals, which makes the large dispersion in valence band (VB). This is beneficial for the mobility of holes promoting high photocatalytic activity [3–5].

Secondly, the structure has a high openness because of the oxygen vacancies in  $\text{Bi}_2\text{O}_3$  lattices. It has an intrinsic vacancy concentration (25%) on the highly disordered oxygen sublattice. It

has been confirmed that the structure-openness in a semiconductor could provide ample space for momentary polarizing charge. This effect further accelerates the charge separation between the photo-created holes and electrons and consequently enhances the photocatalytic reactions [6].

Thirdly, among four polymorphic phases of  $\text{Bi}_2\text{O}_3$ ,  $\alpha$ -,  $\beta$ -,  $\gamma$ -formations present a low electrical conductivity, however,  $\delta$ -phase presents very high ionic conductivity [7]. This is an incomparable advantage of  $\delta$ -phase  $\text{Bi}_2\text{O}_3$ , i.e., the highest oxygen ionic conductivity ( $\sim 1$  S/cm at 1023 K). This value is more than two times higher than the well-known electrolyte of yttrium-stabilized zirconia (YSZ) [8]. And this unusually high ionic conductivity is ascribed to the high structure-openness mentioned above together with high polarizability of Bi- $6s^2$  lone pairs. The good conduction of a semiconductor is beneficial for the easy movement of electrons or holes in the process of photocatalysis. However,  $\delta\text{-Bi}_2\text{O}_3$  is a meta-stable phase, which is only stable in a narrow temperature 730–825 °C [9]. This is the reason for the limitation of the practical application.

In present work,  $\text{Bi}_{14}\text{MoO}_{24}$  was developed and evaluated by incorporating Mo(VI) into  $\delta\text{-Bi}_2\text{O}_3$ . Mo implies the significant lowering of the symmetry from the fluorite-type O sublattice. This

\* Corresponding author.

E-mail address: [zhengmin@suda.edu.cn](mailto:zhengmin@suda.edu.cn) (M. Zheng).

derives a bismuth-rich  $\text{Bi}_{14}\text{MoO}_{24}$  with lower tetragonal lattices than the defect cubic fluorite-type structure of  $\delta\text{-Bi}_2\text{O}_3$ .  $\text{Bi}_{14}\text{MoO}_{24}$  was reported to be a fluorite-type superstructure ( $\delta\text{-Bi}_2\text{O}_3$ ) with a layered-pseudo pseudo-fcc subcell [10–12]. Ling et al. [13] proposed that  $\text{Bi}_{14}\text{MoO}_{24}$  has octahedral coordination of Mo by O atoms, with each  $\text{MoO}_6$  octahedron having one axial and one equatorial O site vacant. There is also plenty of  $V_o$  in the lattices and Bi–O polyhedral present high distortions because of the steric lone-pair effects. Consequently, high optical absorption and efficient photocatalysis could be expected in  $\text{Bi}_{14}\text{MoO}_{24}$ .

$\text{Bi}_{14}\text{MoO}_{24}$  was synthesized by the facile co-precipitation route. The phase formation and the Rietveld refinement were finished. The surface and microstructure were investigated by SEM, EDS, TEM, and BET measurements. The photocatalytic behaviors were measured on degradation of Rhodamine B (RhB) by visible irradiation. XPS, photoluminescence and decay lifetimes were measured to elucidate the photocatalytic activity.

## 2. Experimental

$\text{Bi}_{14}\text{MoO}_{24}$  was prepared by co-precipitation route.  $\text{Bi}(\text{NO}_3)_3 \cdot 5\text{H}_2\text{O}$  (Junsei Chemical Co., 99.0%) and  $(\text{NH}_4)_6\text{Mo}_7\text{O}_{24} \cdot 4\text{H}_2\text{O}$  (Junsei Chemical Co., 99.0%) with the molar ratio of 14:1 were used as the starting materials. In a typical synthesis,  $\text{Bi}(\text{NO}_3)_3 \cdot 5\text{H}_2\text{O}$  (4.85 g) and  $(\text{NH}_4)_6\text{Mo}_7\text{O}_{24} \cdot 4\text{H}_2\text{O}$  (0.2 g) were dissolved in 100 mL and 50 mL water, respectively. The two solutions were mixed together under strong stirring. The mixture was further stirred for 60 min at 80 °C with magnetic stirring. Then the solutions were slowly added in the mixture of  $\text{NH}_3 \cdot \text{H}_2\text{O}$  (1 mol/L) with strong stirring. The precipitation could be found in the solutions, which was then aged, filtrated and washed with hot water. The powders were dried at 100 °C for 6 h, and the precursors were obtained. The final  $\text{Bi}_{14}\text{MoO}_{24}$  products could be obtained by calcining the precursor at 650 °C in 2 h. The reference sample of  $\text{Bi}_2\text{O}_3$  was prepared in the same method.

XRD patterns were taken on a Rigaku D/Max (Rigaku Corporation, Tokyo, Japan) diffractometer (40 kV, 30 mA), and the incident X-ray radiation was created from a Cu  $K\alpha$  target. A UV–vis–NIR spectrophotometer (Cary 5000, 175–3300 nm) was applied to measure the optical absorption spectra. The morphologies of SEM and TEM were investigated on S-4800 (Hitachi Ltd., 15 kV) scanning electron microscopy and an electron microscope (JEM-2100, JOEL Ltd., 200 kV), respectively. The emission and decay were measured under excitation of a pulsed Nd:YAG laser (355 nm, Spectron Laser System SL802G). LeCroy 9301 oscilloscope was applied to collect the data of the emission and decay.

The photocatalytic activities of the samples were conducted for the photo-degradation of the methylene blue ( $10 \text{ mg L}^{-1}$ , 300 mL) and the colorless phenol ( $\text{C}_6\text{H}_5\text{OH}$ ) solutions ( $100 \text{ mL}$ ,  $20 \text{ mg L}^{-1}$ ). A 500 W Xe lamp was used the irradiation source. The excitation was the light with the wavelength longer than 420 nm by arranging an optical filter before the lamp. The air-flow was input the photocatalytic reactor by a pump with the rate at  $500 \text{ mL min}^{-1}$ . Typically, in a photocatalytic test, 0.05 g  $\text{Bi}_{14}\text{MoO}_{24}$  sample was used in 300 mL of RhB ( $10 \text{ mg L}^{-1}$ ) dye solution. The reaction system was put in a dark place about 1 h to reach desorption/adsorption equilibrium before the test. 5 mL RhB solution was extracted from the reactor at 15 min interval to measure absorption spectra.

## 3. Results

### 3.1. Crystal formation

The XRD pattern of  $\text{Bi}_{14}\text{MoO}_{24}$  nanoparticles was measured to identify the phase formation as shown in Fig. 1. The pattern could

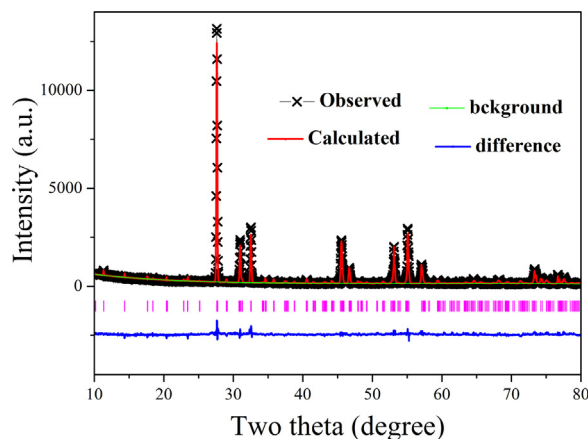


**Fig. 1.** The calculated (red line), observed (black cross), difference (bottom) of the XRD in the Rietveld structure refinement of  $\text{Bi}_{14}\text{MoO}_{24}$ . (For interpretation of the references to color in this figure legend, the reader is referred to the web version of this article.)

**Table 1**

The refined crystallographic parameters of  $\text{Bi}_{14}\text{MoO}_{24}$ .

Formula	$\text{Bi}_{14}\text{MoO}_{24}$
Radiation	Cu $K\alpha$
$2\theta$ range (°)	10–80
Symmetry	Tetragonal
Space group#	14/m (87)
a/Å	8.6932 (11)
b/Å	8.6932 (11)
c/Å	17.2894 (26)
$\alpha/^\circ$	90
$\beta/^\circ$	90
$\gamma/^\circ$	90
Z	2
$R_p$	0.0982
$R_{wp}$	0.1053
$\chi^2$	17.41
V	1306.59 (50) Å <sup>3</sup>

be well indexed to the standard card PDF#49-0281 for  $\text{Bi}_{14}\text{MoO}_{24}$ . No impurity peak was detected. To investigate detailed structural characteristics, the experimental XRD patterns were conducted by Rietveld refinement on the GSAS program shown in Fig. 1. The refinement gave residual errors of 9.82% and 10.53% for  $R_p$  and  $R_{wp}$ . The refined unit cell data and the atomic structural coordinates are listed in Tables 1 and 2, respectively. The bismuth molybdate has in a tetragonal structure with a space group of 14/m (87). The unit cell parameters are  $a = 8.6932(11) \text{ \AA}$ ,  $c = 17.2894(26) \text{ \AA}$ ,  $\alpha = 90^\circ$ ,  $Z = 2$  and  $V = 1306.59(50) \text{ \AA}^3$ .

$\text{Bi}_{14}\text{MoO}_{24}$  is related to that the face-centered cubic (fcc)  $\delta\text{-Bi}_2\text{O}_3$ -like structure (see supporting information Fig. S1). It has been reported that the fcc  $\delta$ -phase of  $\text{Bi}_2\text{O}_3$  undergoes a transformation into one of two metastable phases, i.e.,  $\beta$ -phase (tetragonal) and  $\gamma$ -phase (bcc), before reverting to the monoclinic stable form [14]. The lattices contain three kinds of Bi ions in a layer structure, i.e., Bi1 (8h), Bi2 (16i), Bi3 (4e). Bi(1) plus Mo form cationic layers  $z+0$ ,  $1/2$  and Bi(2) plus Bi(3) at  $z+1/6$ ,  $1/3$ ,  $2/3$ ,  $5/6$ .  $\text{Bi}^{3+}$  ions in  $\text{Bi}_{14}\text{MoO}_{24}$  show the different surrounding from the fluorite-type matrix [13]. There are three type of Bi–O polyhedral in  $\text{Bi}_{14}\text{MoO}_{24}$  lattice. Bi(2) loses two adjacent and one opposite O atoms to create a distorted square pyramid; Bi(1) loses two adjacent O atoms to induce a distorted trigonal prism; while, there are eight O atoms coordinated with Bi(3) site [13]. The geometries suggest the existence of a lone pair with partial  $p$ -character at the metallic center.

Note that in Rietveld refinement,  $O_1$ ,  $O_2$  are 1/2 occupied while  $O_3$  is 3/4 occupied. Meanwhile the distance between Bi1–Bi2

Download English Version:

<https://daneshyari.com/en/article/6448886>

Download Persian Version:

<https://daneshyari.com/article/6448886>

[Daneshyari.com](https://daneshyari.com)